J. Nano Struct., 5(3): 251-256, Autumn 2015
DOI: 10.7508/jns.2015.03.006

ORIGINAL RESEARCH PAPER

Fabrication and Electrochemical Behavior of Monoclinic CuO and CuO/Graphite Composite Nanoparticles as Cathode in an Alkaline Zn-CuO Battery

Y. Zeraatkish, M. Jafarian*, M. G. Mahjani

Department of Chemistry, Faculty of Science, K.N. Toosi University of Technology, P.O. Box 15875-4416, Tehran, Iran

Article history:
Received 20/06/2015
Accepted 03/08/2015
Published online 01/09/2015

Keywords:
CuO
Electrochemical impedance Spectroscopy (EIS)
Graphite
Monoclinic structure

**Corresponding author:*
E-mail address:
mjafarian@kntu.ac.ir
Phone: +98 2122853551
Fax: +98 2122853650

Abstract

Electrochemical properties of various rock-shaped-CuO/graphite (G) composites and monoclinic structure CuO nanoparticles as the cathode versus a zinc plate as the anode in a 4M NaOH electrolyte were elucidated by electrochemical impedance spectroscopy (EIS) and chronopotentiometry (CP) in a two electrode configuration cell. Various values of G 9, 16 and 28 wt% were prepared and studied as cathode materials for an alkaline Zn-CuO Battery. The EIS results demonstrated that increasing the mass ratio of G caused significant decrease in charge transfer resistance (Rct) and capacitive behavior of the electrode. Also, the discharging voltage of the cells was increased due to raising the mass ratio of the graphite. Besides, electrochemical properties of the monoclinic structure CuO nanoparticles as cathode material in the alkaline battery was compared with a rock shaped CuO particles. The results showed that the discharged voltage of monoclinic CuO nanoparticles is less than another rock shaped CuO nanoparticles form.

1. INTRODUCTION

Today's increasing needs for energy storage tools cause researchers look for variety of low cost energy storage systems to response these demands of the modern world. Beside the discovery of new energy storage systems, modification of previous systems is an approach to making them more efficient. Metal oxides are one of the using materials in the batteries[1, 2]. Low conductivity of these materials causes a decrease in efficiency of the batteries by rising over potential of the electrodes. So, they are merged with high conductive electrochemical inert materials like activated carbon,[3] carbon nanotubes, graphene, acetylene black and graphite[4] to reduce the

electrodes over potentials and increase specific energy and capacity of the batteries.

CuO is used in variety types of batteries. CuO is considered as both anode[5] and cathode[6-9] materials for Li batteries. Park et al. used CuO Hollow Nanostructures as Anode Materials for Lithium-Ion Battery. [5] The efficiency of copper oxide as electrode in Li ion batteries depends on its size and crystallographic structure. Gao et al. stated that the fine and polycrystalline CuO nanorods as anode materials for Li ion battery show higher electrochemical capacity than for the single crystalline bulk nanorods because of their large surface area and various physical defects. [10] Also, a previous report using CuO as cathode material stated that the morphology of the cathode material considerably influences the discharge performance of the battery[6]. In this study CuO as cathode electroactive material was merged with variety amounts of graphite and alterations in the electrochemical behavior of cathode were elucidated parallel to variation in the graphite value. CuO is one of the semiconductor materials which have electrical resistivity. Therefore its application as electroactive materials to use in energy storage devices is limited by this property. Some conductive materials are used to improvement electrochemical performance of electrode materials i.e. graphite, graphene and so on. Similar to metals graphite has electrical and thermal conductivity. Also, it reveals the properties of a non-metal such as high thermal resistance and inertness. So, graphite is a type of carbon that has the most applications in electrochemical processes[4].

2. Experimental procedure

2.1. Materials and Instruments

The NaOH, graphite and Cu fine powder were Merck products of synthesis grad and used without further purification. Electrochemical measurements were carried out in two-electrode cells containing an electrolyte of aqueous 4M NaOH powered by an EG&G model 273 potentiostat/galvanostat. Galvanostatic discharge experiments were performed at a current density of 500 mAg−1 to measure the electrochemical capacity of the electrode at room temperature. The EIS measurements were performed in the frequency domain of 100 kHz to 20 mHz with amplitude of 5 mV. The X-ray powders diffraction patterns were collected on a Unisantis diffractometer. The field emission scanning electron microscopy (FE-SEM) image was obtained using Hitachi S4160 scanning electron microscope.

2.2. Construction of the electrodes

A large zinc plate with 4×4 cm dimension was used as the counter and reference electrodes, simultaneously. The working (cathode) electrodes were prepared by mixing and pressing CuO, graphite and the binder which is 1% W/W aqueous solution of Carboxymethyl cellulose (CMC). The mass of the CuO on all working electrodes was 0.1g. Various weight ratios of graphite 9, 16 and 28 wt% percent were prepared for construction of the cathode electrodes. Schematic illustration of cathode electrode is presented in Figure 1. A work electrode and the zinc plate were inserted into a beaker containing 4M NaOH to complete the cell.

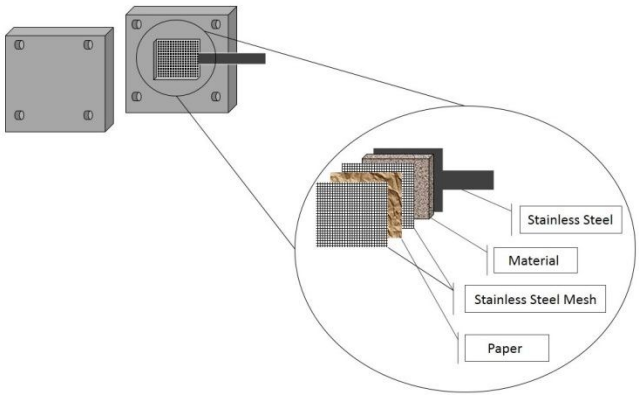

Fig. 1. cathode electrode used for material evaluation.

2.3. Synthesis of CuO

The first sample of CuO particles with the size between 100 and 300 nm was produced by the solid-state thermal oxidation of Cu microparticles(Sample A). For this purpose the Cu microparticles were put in the oven and treated at 500 °C for 7 h. Besides, the second sample, the CuO nanoparticles were synthesized using hydrothermal decomposition of $Cu(OH)_2$ at reflux condition and temperature up to 100 °C. In the procedure, 25 ml of 1.6 M NaOH solution is heated to boiling point. Then, 10 ml $CuCl_2.2H_2O$ (0.1M) solution was added dropwise to the NaOH solution under constant stirring. The solution color is changed from blue-green to dark-brown immediately, signifying that Cu $(OH)_2$ suspension has changed to CuO immediately. After about 30 minutes continuation of reflux condition, the material was separated by filter paper, washed with distilled water and ethanol and dried in oven at 60 °C.

3. Results and discussion

3.1. Physical Characterization

The X-ray diffraction (XRD) pattern of the first prepared CuO sample is displayed in Figure 2. The peaks in the XRD patterns of sample (A) are consistent with the JCPDS 00-044-0706 data of the unknown structure copper oxide. The sample containing NPs indexes to monoclinic CuO (JCPDS number 00-048-1548). However, the diffraction peaks of the NPs are wider than those of another sample, signifying that the earlier consists of smaller crystallites. The Scherrer equation is applied from the XRD patterns to estimate the average crystalline sizes in the CuO samples which are 34 and 29 nm for sample (A) and nanoparticles, respectively.

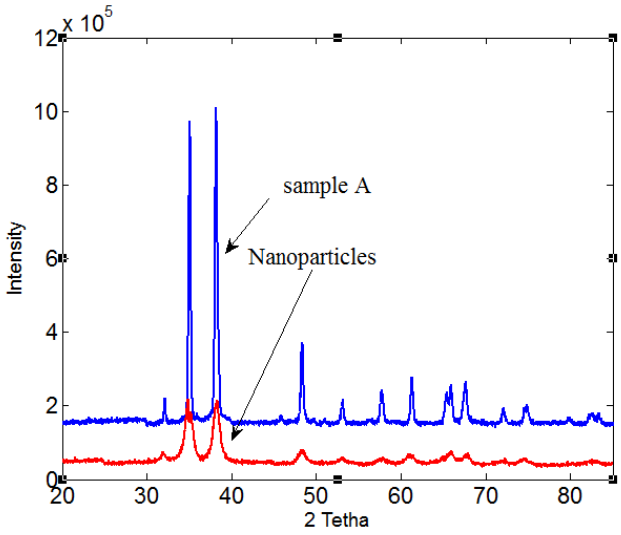

Fig. 2. The XRD patterns of the CuO samples

The morphology and particle size of the samples are considered by FE-SEM. The FE-SEM image in Figure 3a shows rock shaped particles that are between 100 to 300 nm in dimension. Also, Figure 3b shows that the size of NPs is below the 50 nm.

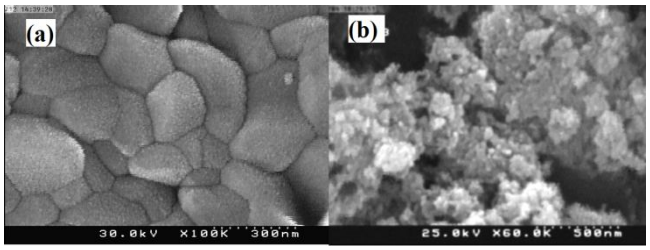

Fig. 3. FE- SEM image of (a): the sample (A), (b): Nanoparticles

3.2. Electrochemical analysis:

Electrochemical impedance spectroscopy

The EIS measurements were done with a two electrode system over the frequency range of 100 kHz–10 mHz at open circuit potential (OCP), in 4.0 M NaOH solution before any discharging of the cells. The electrolyte/interface and associated electrochemical processes is described as an electric circuit in figure 3 comprising of electrical

elements, including constant phase elements (CPE), and resistances. In the circuits Rs, CPE1 and Rct1 indicate solution resistance, a constant phase element corresponding to the double layer capacitance, and the charge transfer resistance of the anode. Also, CPE2 and Rct2 are associated to the double layer capacitance and the charge transfer resistance of the cathode material.

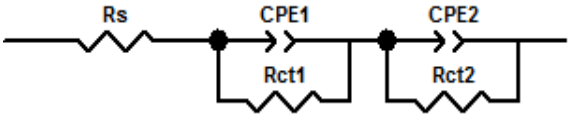

Fig. 4. Extracted equivalent circuit for the EIS results

Figure 5 shows the Nyquist plots of EIS data of four different cathodes which manifested variations of the total charge transfer resistance (Rch1+Rch2). From this figure a significant decrease in the size of the capacitive semicircles are observed, indication for decreasing Rch2 and increasing conductivity due to increasing the mass ratios of the G in the cathode. The Nyquist plots consist of a small semicircle at high frequencies combined to a larger semicircle at the medium to low-frequency limit of the spectrum. The large semicircle can be seen in the Nyquist plots and small semicircle is revealed by the Bode phase plots manifested in figure 6. Two discernible peaks in the Bode plots reveal two semicircles in the Nyquist plots. From the Bode phase plots decreasing the angles at medium frequencies indicates that the capacitive behavior of the electrodes is reduced during increasing the mass ratio of G. Moreover, this figure reveals that monoclinic structure CuO nanoparticles show lower Rct than another structure of CuO particles.

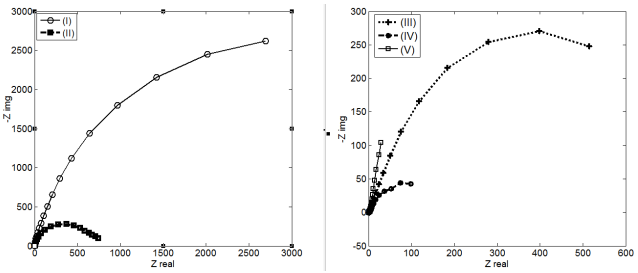

Fig. 5. the Nyquist plots of (I): sample (A), (II): NPs, (III): 9, (IV):16 and (V): 28 wt% G

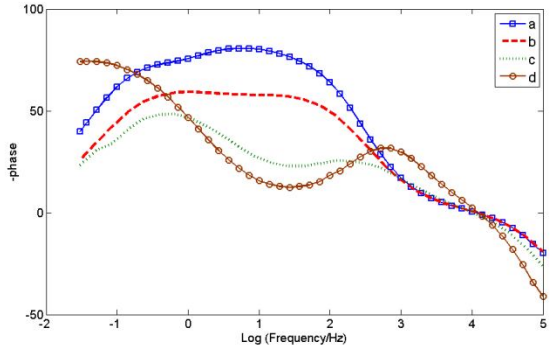

Fig. 6. the Bode-phase plots of the electrodes with different weight ratio of G a: 0, b: 9, c: 16 and d: 28 wt% G

3. 2. 1. Discharge measurements

The discharge cycles of the cells are shown in Figures 7 and 8. The discharge of each cell was achieved without any charging of the electrodes. CuO is discharged at one stage reaction according to equation 1. Also, the electrochemical reaction of the zinc electrode in alkaline

media proceeds via reaction 2.

$$CuO + H_2O + 2e^- \rightarrow Cu + 2\,OH^- \qquad (1)$$

$$Zn + 4\,OH^- \rightarrow Zn(OH)_4^{2-} + 2e^-$$

$$E = -1.199V \qquad (2)$$

It is clear from Figure 7 that the cell containing NPs is unexpectedly discharged at lower potential than the cell containing sample (A) particles. This

may be due to the crystalline type of the particles. So, it can be concluded that monoclinic crystalline structure is not appropriate for use in this kind of battery.

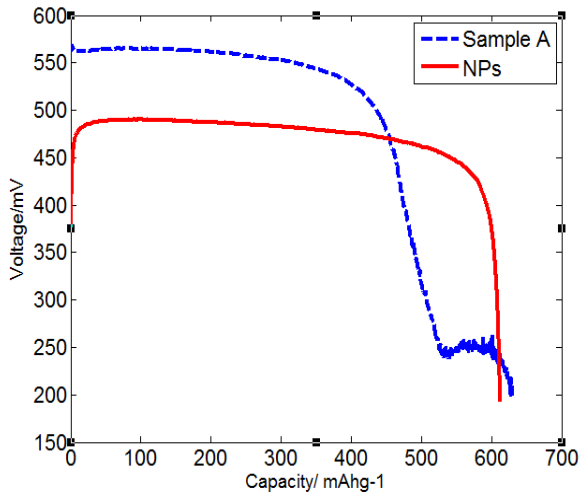

Fig. 7. The discharge cycles of sample (A) and NPs

In continue sample (A) particles were mixed with various amount of graphite and were examined in the same conditions. The discharge results are presented in Figure 8. From this Figure one-stage discharge cycles of CuO, depending on the graphite content, are performed at different potentials. It reveals that the samples with higher amount of graphite are discharged at higher potential. Also, the electrodes with higher value of graphite have more discharge capacity than others .The capacities were calculated on the basis of the weight of CuO only using relation:

$$\text{Capacity} = \frac{it}{3600m} \qquad (3)$$

Where *i* is the discharging current in milliamps, *t* is the time in seconds and *m* is the mass of the CuO.

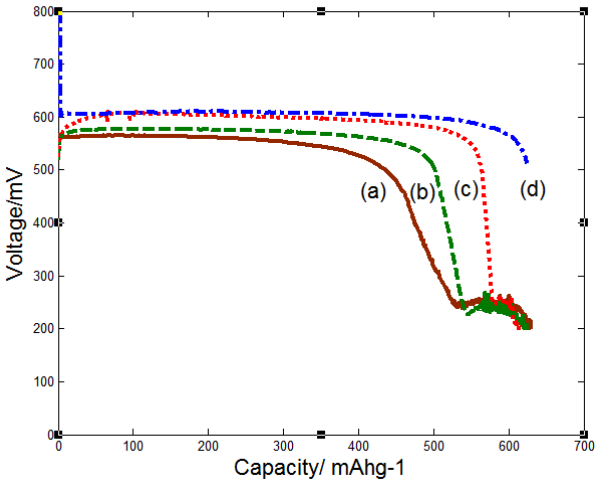

Fig. 8. the discharge curves of the samples a: 0, b: 9, c: 16 and d: 28 wt% G

4. Conclusion

The CuO NPs and another sample of CuO mixed with different amounts of graphite were electrochemically examined in an alkaline condition as the cathode material versus a zinc plate as the anode. The results show that the monoclinic structure NPs are discharged at low potential plateau and adding graphite into CuO electrode not only increases the potential plateau of discharge cycles but also increases the discharge capacity of the cells. Besides, the Rch of the cathode electrode is dramatically decreases due to mixing graphite with electroactive materials.

References

[1] A. Dillon, A. Mahan, R. Deshpande, P. Parilla, K. Jones, S. Lee, Thin Solid Films, 516 (2008) 794-780.

[2] X. Wu, S. Zhang, H. Fang, Z. Du, R. Lin, Chemistry Letters, 43 (2014) 1625-1632.

[3] H. Nagata, Y. Chikusa, Chemistry Letters, 43 (2014) 1335-1336.

[4] M. Wissler, Journal of Power Sources, 156 (2006) 142- 150.
[5] J.C. Park, J. Kim, H. Kwon, H. Song, Advanced Materials, 21 (2009) 803-810.
[6] P. Podhajecky, B. Scrosati, Journal of Power Sources, 16 (1985) 309-315.
[7] P. Novak, Electrochimica acta, 30 (1985) 1687-1692.
[8] P. Novak, B. Klápště, P. Podhájecký, Journal of Power Sources, 15 (1985) 101-108.
[9] P. Novák, Electrochimica acta, 31 (1986) 1167-1173.
[10] X. Gao, J. Bao, G. Pan, H. Zhu, P. Huang, F. Wu, D. Song, The Journal of Physical Chemistry B, 108 (2004) 5547-5554.